Check for updates

Laboratory Tests and Field Surveys to Explore the Optimum Frequency for GPR Surveys in Detecting Qanats

AZADEH HOJAT,[1,2] (iD) HOJJATOLLAH RANJBAR,[1] (iD) SAEED KARIMI-NASAB,[1] (iD) and LUIGI ZANZI[2] (iD)

Abstract—In this paper, we discuss the results of laboratory tests and field surveys using ground penetrating radar (GPR) method to detect qanats at the main campus of Shahid Bahonar University of Kerman (SBUK), Iran. The main purpose of laboratory experiments was to explore the optimum frequency of GPR surveys to detect qanats for the subsoil in the study site. We performed a variety of laboratory tests with a 3 GHz antenna to detect qanats (simulated using dielectric empty targets) hosted by sand with volumetric water content (VWC) values in the range 1.5–8%. The depth to each target was progressively increased until either approaching the edges of the sandbox or modelling a qanat depth for which GPR data could not detect the target anymore. The scaling factors were calculated for each test to estimate the maximum depth of detecting qanats as a function of the scaled GPR frequency. The results showed that in areas where the subsoil is dominated by sand, medium-frequency GPR antennas can penetrate to depths of a few tens of meters, but the penetration depth considerably decreases when the soil moisture and/or clay content of the medium increase. Based on the results of laboratory simulations, qanats are detectable at a maximum normalized depth of about 15–17 times of the wavelengths in very dry sands with VWC less than 5% while the detectable range rapidly drops down to less than 3 or 4 times of the wavelengths in more humid sands with VWC of about 8%. We also discuss the results of a few field GPR surveys that were measured using antennas with the 50 MHz and the 250 MHz frequencies in the northwestern part of the study area. The processed GPR images could detect a qanat in the position compatible with the results of previous remote sensing studies performed in the area. The depth to the detected qanat is 13.5 m, which is a little bit beyond the maximum limit predicted by the laboratory tests.

Keywords: Qanat, water infrastructures, GPR, optimal frequency, volumetric water content, remote sensing, aerial photos.

[1] Department of Mining Engineering, Shahid Bahonar University of Kerman, Jomhouri Boulevard, Kerman 76188, Iran.
[2] Dipartimento di Ingegneria Civile e Ambientale, Politecnico di Milano, Piazza Leonardo da Vinci 32, 20133 Milan, Italy. E-mail: luigi.zanzi@polimi.it

1. Introduction

Qanat system is mostly believed to have been invented in Iran some thousands of years ago to tap groundwater from mountain areas and conduct it to less elevated lands (e.g., Goblot, 1979; Kobori, 1964; Semsar Yazdi & Labbaf Khaneiki, 2017). Eleven Persian qanats have been inscribed on Unesco's world heritage list as a testimony to civilization and cultural traditions of living in desert areas (www.unesco.org, last visited in 2021). Arid and semi-arid areas of Iran such as Kerman, Khorasan, and Yazd Provinces host a large number of qanat networks. The geographical distribution of qanats through history is discussed by Semsar Yazdi and Labbaf Khaneiki (2017). Qanats are distributed not only in arid and semi-arid regions of the world with shortage of surface streams and rich groundwater resources, but they are also found in some rainy regions. Qanat system was spread from Iran to Afghanistan, Pakistan, Iraq, Oman, Saudi Arabia, Syria, Azerbaijan, India, Japan, China, Egypt, Libya, Tunisia, Algeria, Morocco, Mexico, Peru, Chile, Hawaii, USA, Spain, Greece, Germany and Sicily (Semsar Yazdi & Labbaf Khaneiki, 2017).

A schematic illustration of qanat system is shown in Fig. 1a. The underground gallery of a qanat system transfers water only by gravity. This gallery is connected to the ground surface with vertical shafts. The first well, which penetrates deeper than the water table, is known as mother well. The gallery dimensions were such that the workers could go through and work in it: a height in the range 90-150 cm and the width about half the height (Semsar Yazdi & Labbaf Khaneiki, 2017). Water transferred by the qanat gallery exits at ground surface at the qanat
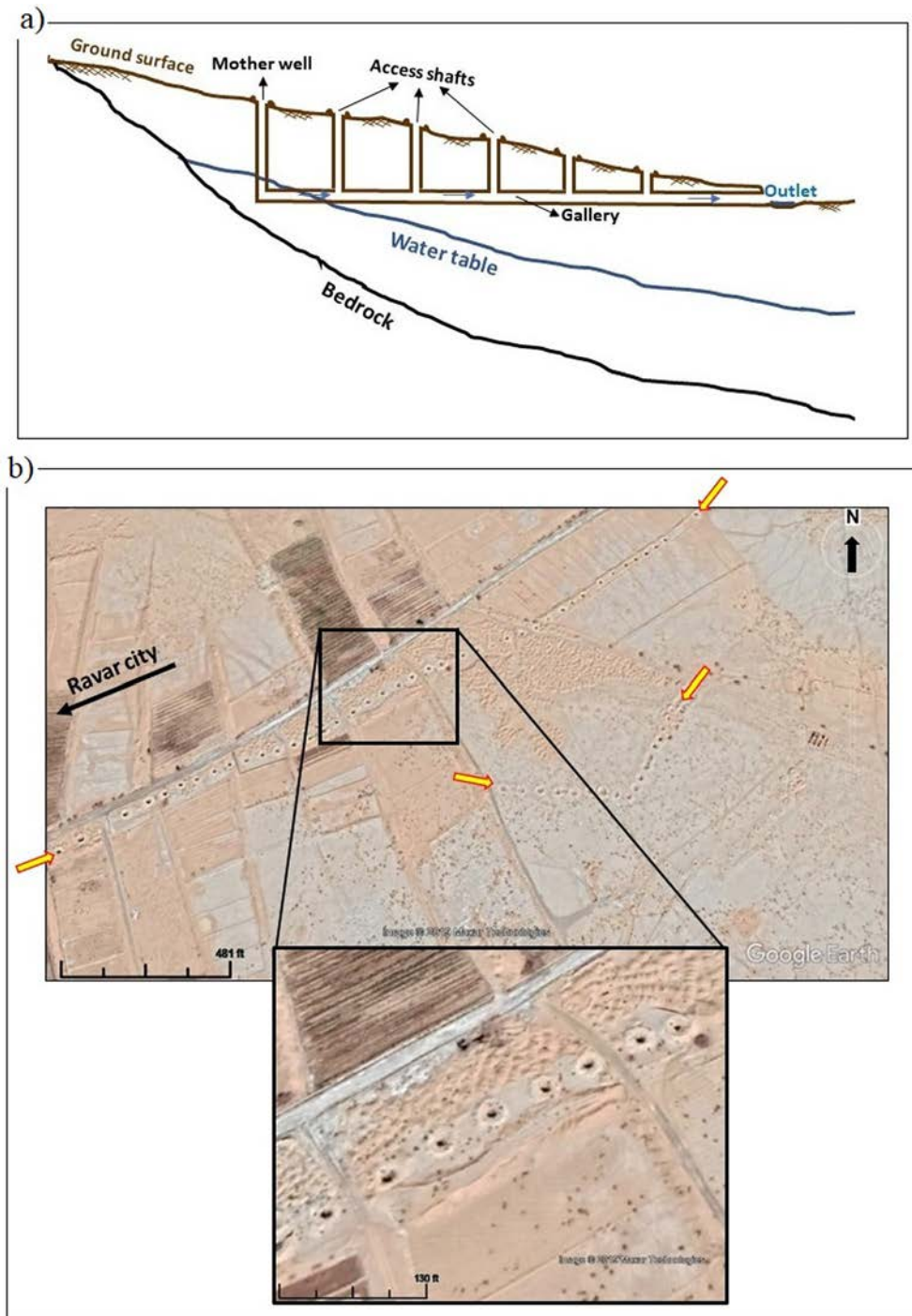
Figure 1
a Schematic section of a qanat system. **b** Yellow arrays track vertical shafts of qanat systems arriving at agricultural lands east of Ravar city in Kerman Province (from Google Earth)

outlet. Figure 1b illustrates an example of surface track of qanat shafts arriving at agricultural lands east of Ravar city in Kerman Province.

Qanats were gradually abandoned in most cities as a result of changes in water supply systems and uncontrolled development of urban areas. Rapid construction projects rarely included proper management of qanat systems and usually ignored keeping a record of qanat galleries. In the recent decade, geotechnical problems such as land subsidence and cracks in buildings have continued to occur in areas where qanat galleries run beneath. Therefore, there has been an increasing need to develop methods capable of mapping qanat galleries (Hojat et al., 2019b, 2020).

Mapping qanats in detail is a challenging problem for any individual geo-engineering technique. Integration of different techniques is an optimum solution to overcome the limitations of any individual method to map qanats in detail (Hojat et al., 2018). Remote sensing studies fall among the efficient methods to study qanats at the initial stages and are helpful to track qanats on the surface. All three methods of optical, radar and lidar remote sensing can usually be used to study qanats, because the surface characteristics of qanats allow them to be mapped well in all these methods. However, the issues related to high costs and the fact that some qanats cannot be observed on the ground for any reason lead us to refer to old aerial photos. Under normal conditions, both high-resolution satellite images and aerial photos can be used. Recently, the topic of unmanned aerial vehicle (UAV) images has become very hot and these images can be used with great accuracy. UAV images have the advantage that a digital elevation model (DEM) can be also produced in addition to the images. From the DEM, it is possible to estimate the volume of the soil extracted out of the shaft, and thus, an approximate depth to qanat can be estimated. Based on the results of remote sensing studies, optimized geophysical surveys can be designed to map the subsurface galleries of qanat systems. Among different geophysical methods, electrical resistivity tomography (ERT), ground penetrating radar (GPR), and gravimetry are the most common methods used to map subsurface cavities (e.g., Rousset et al., 1998; Beres et al., 2001; Kofman et al., 2006; Mochales

et al., 2008; Loke et al., 2013; Park et al., 2014; Harun & Samsudin, 2014; Alsharahi et al., 2019; Lyu et al., 2020; Tresoldi et al., 2020; Hojat et al., 2021, 2023; Porzucek & Loj, 2021). In this paper, we study the response of GPR method to detect qanats with the main purpose to study the challenge of penetration depth that GPR surveys suffer regarding different antenna frequencies. It is well known that the GPR method has the highest resolution among the geophysical methods and it can be used in a variety of applications thanks to its capability to detect both metallic and non-metallic targets (e.g., Arosio et al., 2018, 2020; Benedetto et al., 2017; Conyers, 2013; Hojat et al., 2019a; Izadi-Yazdanabadi et al., 2022; Maierhofer & Leipold, 2001; Valle & Zanzi, 1998; Zanzi et al., 2019). For what concerns qanat investigations, GPR method has the demanded high resolution to detect the target and it is especially an efficient method in urban areas where dense construction of buildings and roads prevents application of the ERT method. However, GPR method suffers from the limited penetration depth especially in areas where the subsoil tends to be more conductive.

In this study, we have performed a variety of laboratory tests with a high frequency antenna (3 GHz) to explore the challenges in the penetration depth of GPR method when exploring qanats hosted by dry to low-moisture sands. The qanat target was simulated with small dielectric empty cylinders of different sizes embedded in relatively small sand boxes. The results were extrapolated to predict the expected detection capabilities in real situations by applying the corresponding scaling factor (i.e., the ratio between cylinder size and real qanat size) to both frequency and detection range. The theoretical background of this approach consists of the well-known radar equation (Levanon, 1988) that, in a lossless medium, relates the ratio between the received and the transmitted power to the gain and effective area of the antennas, to the radar cross section of the target and to the antenna to target distance. Radzevicius and Daniels (2000) discussed the scattering properties of a dielectric cylinder embedded in a medium with higher permittivity (like a void cylinder in a sandy soil) showing that the normalized scattering width (i.e., the 2D radar cross section normalized to the wavelength) is a function of

the normalized size of the cylinder, i.e., of the ratio of the radius to the wavelength. As a result, the ratio between the received and the transmitted power for a dielectric cylinder in a lossless medium is a function of two normalized parameters, i.e., the normalized size of the cylinder and the normalized antenna to target distance. Therefore, the results observed with small scale high frequency laboratory tests can be easily rescaled to predict the results at the real site scale with lower frequencies. Later, we also present the results of a few GPR profiles that were measured in the study site and we compare the observed detection range with the laboratory-based prediction.

2. The Study Site

This study is part of a project focused on geophysical and geotechnical studies to construct a geophysics-geotechnics test site of natural qanats at the main campus of Shahid Bahonar University of Kerman (SBUK), southeast of Iran. Aerial photos and historical notes prove that several qanat systems pass below the land where the main campus of the university was constructed. In recent years, subsidence problems and cracks of some building walls initiated the need to locate these qanat systems (Hojat et al., 2018). Figure 2a illustrates the results of remote sensing studies that could track qanat systems from old aerial photos of the university campus. Considering the fact that qanat shafts are not visible on the surface because they are completely covered by soil, asphalt and buildings in most parts of the study site, old aerial photographs taken in 1992 were used. These images were first filtered using a high-pass filter (Fig. 4). The qanats were then drawn after applying geometrical correction in the geospatial information system (GIS) (Figs. 2a and 4). The results were validated through field visits where some vertical shafts are still present at the non-developed areas of the university campus in its southeastern part (Fig. 2b). We could measure depths varying in the range 6-20 m by direct observations in some of these shafts.

ERT and GPR investigations are proposed to confirm the subsurface qanat galleries and determine their depths at the study site. Considering that many buildings and connection roads are present in most parts of the university campus, GPR measurements are the preferred method due to the feasibility of the method in such a study area. The subsoil at the study area is mainly dry sand, which falls among the favorable materials for GPR where penetrations of a few tens of meters are achievable at low frequencies (Francke et al., 2009; Zanzi et al., 2019).

3. GPR Measurements

3.1. Laboratory Measurements

GPR method usually has the required resolution to detect qanats, but it is challenged by limited depth of penetration for deep qanats in radar absorbing soils. We performed small-scale laboratory measurements to predict the GPR performances at the field scale.

To simulate qanats in the laboratory, a variety of dielectric empty targets were used. These objects were placed in sand as the hosting material. The volumetric water content (VWC) of sand in different tests varied in the range 1.5–8%. Data acquisitions were performed along profiles (red arrows in Fig. 3) that were perpendicular to the strike of qanats and a 3 GHz IDS antenna was used in all measurements. We selected this high frequency antenna so that small sand boxes with their maximum size in the order of one meter would be large enough to reproduce several down scaled versions of the qanat problem. Figure 3 shows examples of our laboratory experiments. For the example shown in Fig. 3a, three dielectric empty cylinders with different diameters (corresponding to different scaling factors) were placed at the bottom of the sand box. To simulate different burial depths, the sand was gradually added above these objects until completely filling the box. At each step, GPR profiles were measured above the sand layer to study how the targets would be detected at each depth. Figure 3b shows an example of the tests in which the targets were placed vertically to be able to use the longer side of the sand box in order to simulate larger depths. In these tests, the targets were moved in the lateral direction to simulate greater depths. For example, for the cylindrical object in Fig. 3b, we started from burying the object almost in the middle of the box and it was progressively moved farther from GPR antenna side (yellow arrow). For all
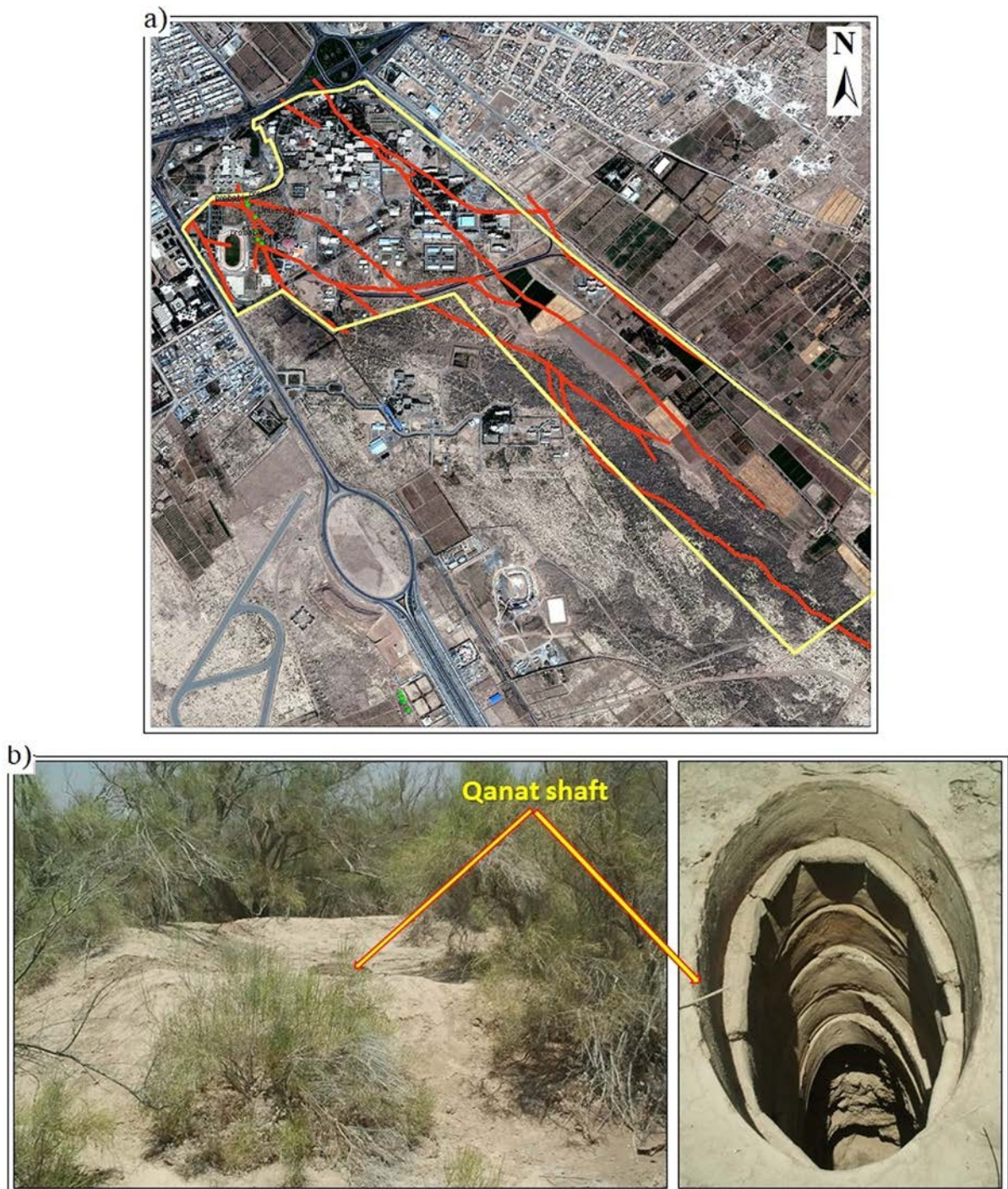
Figure 2
a The main campus of SBUK (yellow line) located in Kerman Province, southeast of Iran. Red lines indicate qanat systems tracked by previous remote sensing studies (Hojat et al., 2018). **b** Examples of qanat shafts observed at SBUK during the field visit in the southeastern part of the campus where construction projects have not been developed yet
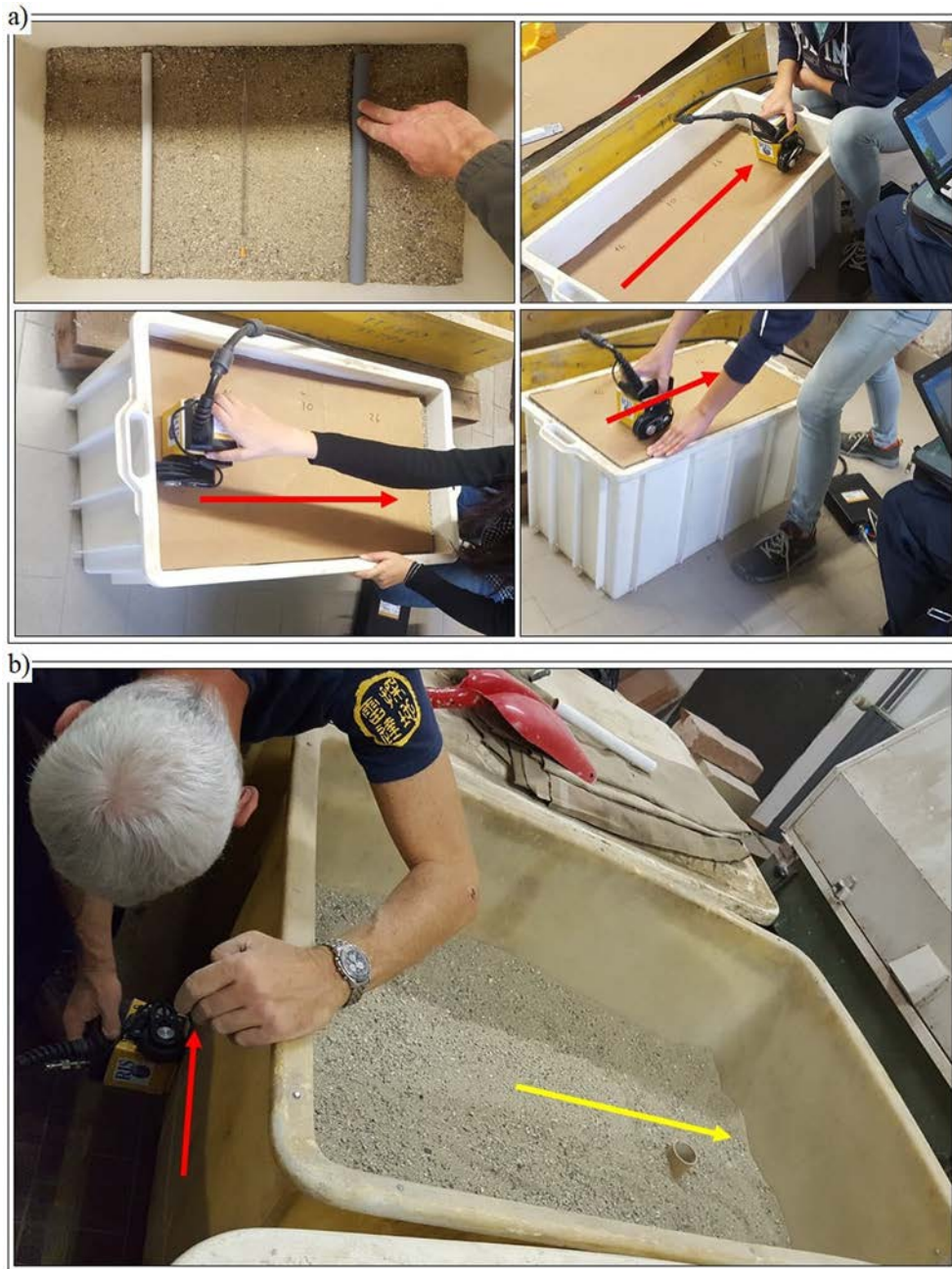
Figure 3
Examples of GPR tests to detect qanats (cylindrical targets) at different depths: **a** The targets were covered with different heights of sand and GPR profiles (red lines) were measured perpendicular to the strike of the buried objects. **b** An example of targets placed vertically to simulate larger depths using the longer side of the sand box. GPR profiles were measured along the red line and the target depth was progressively increased along the yellow arrow

these laboratory measurements, we set up a minimum sampling frequency of 20 GHz and a spatial sampling interval of 2 mm or 4 mm.

3.2. Field Measurements

In this paper, we present a few examples of GPR surveys that were performed in the northwestern part of the university campus. The selected GPR profiles were measured using MALÅ antennas with the frequencies of 50 MHz (profile 1 on Fig. 4) and 250 MHz (profiles 2 and 3 on Fig. 4) and they pass over an expected qanat system that was detected based on the results of remote sensing studies (Fig. 4). We present these GPR surveys with the aim to confirm the results of remote sensing studies and in the case of success to better locate the lateral position and depth of qanats. The 50 MHz data were

Figure 4
Top: Example of qanat shafts that are well observed on old photographs of the study site. The right photo has been high pass filtered. Bottom: Zoomed view of the northwestern part of the study site where two qanats (red lines) are tracked from remote sensing studies (Hojat et al., 2018). Profile 1 was measured with a 50 MHz antenna and profiles 2 and 3 were measured in the opposite directions with a 250 MHz antenna

measured with a sampling frequency of about 750 MHz and a spatial sampling of 30 cm while for the 250 MHz data we used a sampling frequency of 3 GHz and a spacing of 5 cm.

4. Results and Discussion

4.1. Laboratory Tests

Laboratory data were processed applying a standard processing procedure including a gain function to compensate absorption and divergence. In all tests, the velocity of the radar wave in sand was also measured.

Figure 5 shows the results for the test illustrated in Fig. 3a. In this test, three cylindrical targets A, B, and C with respective diameters of 1.6 cm, 1 cm, and 2.5 cm were buried in sand with VWC = 4.8%. The first profile was measured over the sand thickness of 20 cm above the targets. Two other measurements were performed with the burial depth of 26 cm and

30 cm (the maximum possible depth in this test) for targets. Considering a typical diameter of 1 m for qanats, the scale factors for A, B, and C targets are 1/62.5, 1/100 and 1/40, respectively. As can be seen on the processed images shown in Fig. 5, all targets are detectable up to the maximum explored depth of 30 cm. This suggests that a 48 MHz antenna might detect qanats at the depth of 19 m depth, a 30 MHz antenna might detect qanats at the depth of 30 m, and a 75 MHz antenna might detect qanats at the depth of 12 m. Of course, the expected depth of penetration would greatly decrease as the VWC and/or clay content of the sand increases.

The results of another test in which qanats were detected in all measurements are shown in Fig. 6. In this test, two empty targets A and B with a 4 cm square section and a 2.5 cm circular section, respectively, were buried in dry sand with VWC = 2.5%. The sand thickness was progressively increased from 30 cm up to the maximum height of the box (about 50 cm). The scale factors for A and B targets in this
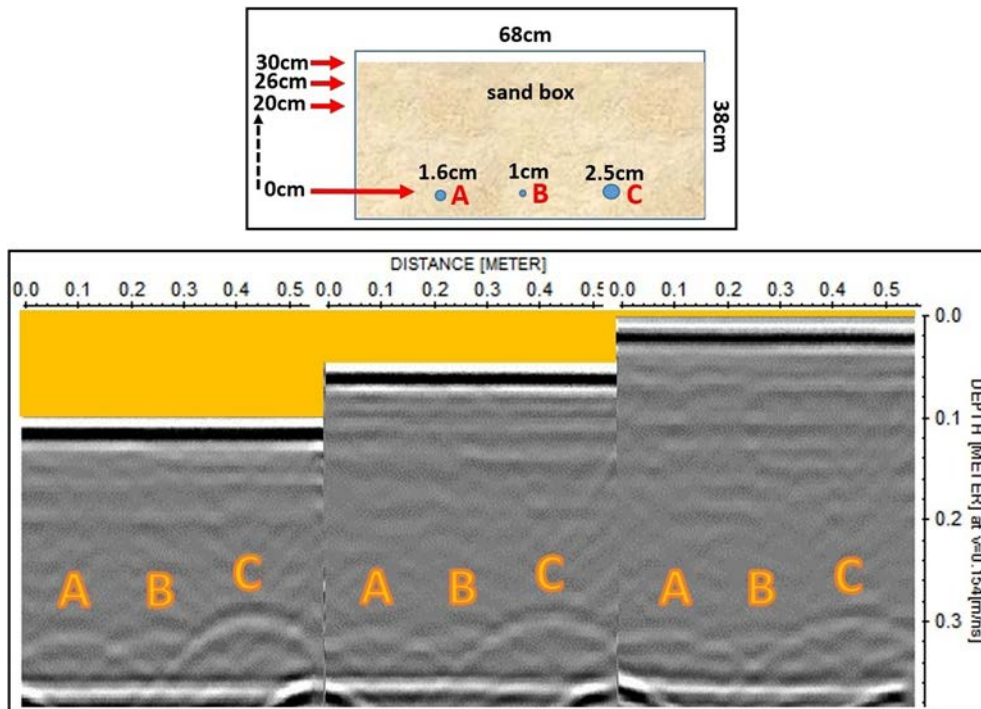

Figure 5
GPR tests on dry sand with VWC = 4.8%. **A**, **B**, and **C** are empty cylindrical targets. Sand thickness above the targets was increased from 20 to 30 cm. The targets are detectable in all GPR images
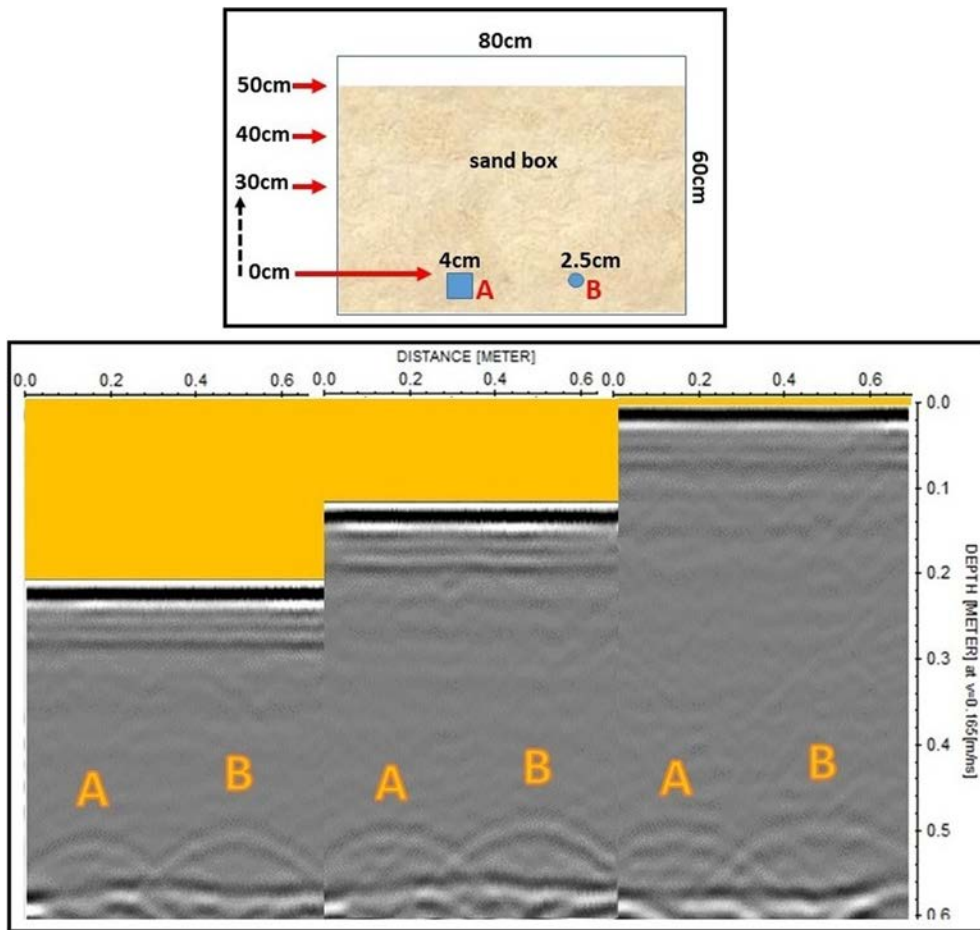
Figure 6
GPR tests on dry sand with VWC = 2.5%. **A** and **B** are empty targets with a 4 cm square section and a 2.5 cm circular section, respectively. Sand thickness above the targets was progressively increased from 30 cm to about 50 cm. Both targets are detectable in all GPR images

test are 1/25 and 1/40, respectively. Detection of both targets in all the processed GPR images shown in Fig. 6 suggests that a 120 MHz antenna might detect qanats at 12.5 m depth while a 75 MHz antenna might detect qanats at 20 m depth. Note the expected penetration depth obtained from this test for target B compared to the target C in the previous example. The two targets have the same scale factor and they are embedded in almost dry sand (VWC = 4.8% in Fig. 5 and VWC = 2.5% in Fig. 6). This suggests the possibility to extend the predictable detection range of qanats to 20 m with a 75 MHz antenna.

Figure 7 illustrates the results of tests in which the targets were displaced laterally in the sand box to move them farther from the antenna side (see Fig. 3b

as example). The VWC of the sand used in these tests was 1.5%. In most of these measurements, the targets arrived at depths far enough not to be detectable on GPR images.

The target used in Fig. 7a is a cylindrical object with the diameter of 8 cm. It was put at depths 34 cm, 57 cm, 85 cm, 95 cm, and 105 cm. As can be seen in the figure, the corresponding GPR images of this test could detect the object down to 95 cm but the anomaly is lost when moved to the depth of 105 cm. The scale factor for this test is 1/12.5, which suggests that the maximum depth to be able to detect a qanat in very dry sand using a 240 MHz antenna would be 12 m.
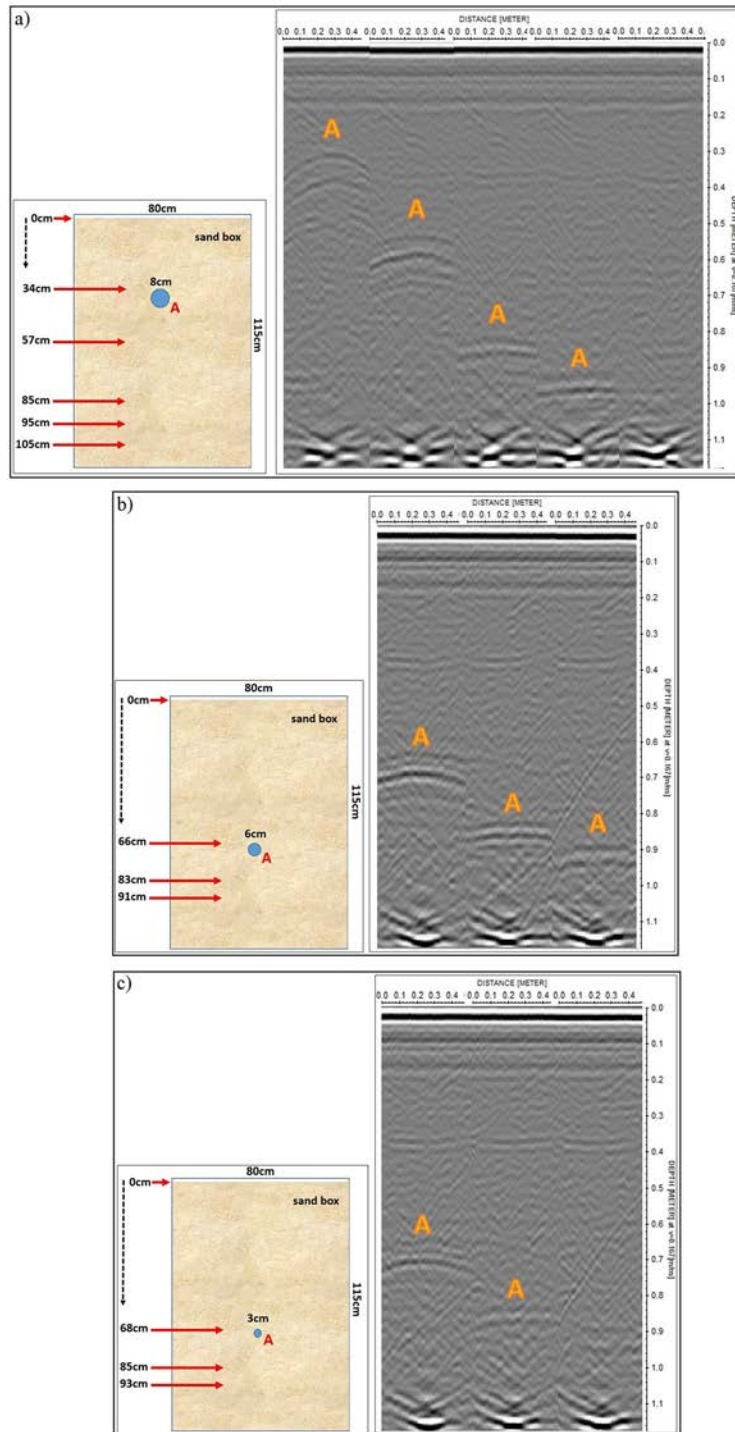
Figure 7

GPR tests on dry sand with VWC = 1.5%. **a** A cylindrical target with the diameter of 8 cm was detected down to the depth of 95 cm and it was not detected when buried at 105 cm. **b** A cylindrical target with the diameter of 6 cm was detected down to the depth of 91 cm. **c** A cylindrical target with the diameter of 3 cm was detected down to the depth of about 85 cm and it was not detected when buried at 93 cm

Figure 7b shows the results for the test shown in Fig. 3b where a cylindrical object with the diameter of 6 cm was used. The object was placed at distances of 66 cm, 83 cm, and 91 cm from the antenna side. All the processed images shown in Fig. 7b have clearly detected this object. Therefore, with the scale factor 1/16.7, these measurements show that using a 180 MHz antenna, qanats at the depth of 15 m might be still detected.

The third target used in these measurements was a cylindrical object with the diameter of 3 cm, which was placed at distances 68 cm, 85 cm, and 93 cm from the antenna (Fig. 7c). As can be seen on the processed images, this object was detected at the depth of 85 cm, but it was not detectable at the depth of 93 cm. The scaling factor of 1/33.3 for this object suggests that using a 90 MHz antenna, qanats could be detected at a maximum depth of 28 m as far as the hosting material is very dry.

Another interesting test was performed using targets buried in the sand with VWC = 8%. In this test, two empty targets A and B with a 1 cm square section and a 2.5 cm circular section were buried at the bottom of the sand box and the thickness of the sand above the targets was progressively increased until target A and then target B were not detectable on GPR images (Fig. 8). The base of the sand box in this test was curved and its corresponding reflection is well recognized on GPR images. As can be seen in Fig. 8, both targets are detected when buried at the depth of 15 cm. Increasing the sand thickness over the targets to 21 cm, target A, which is smaller, is no longer detectable, but target B is still detected. When the depth of burial was increased to 27 cm, target B was also missed on GPR images. The scale factors for A and B targets in this test are 1/100 and 1/40, respectively. It can be concluded that a 30 MHz antenna might detect qanats down to a maximum depth of 15 m and a 75 MHz antenna
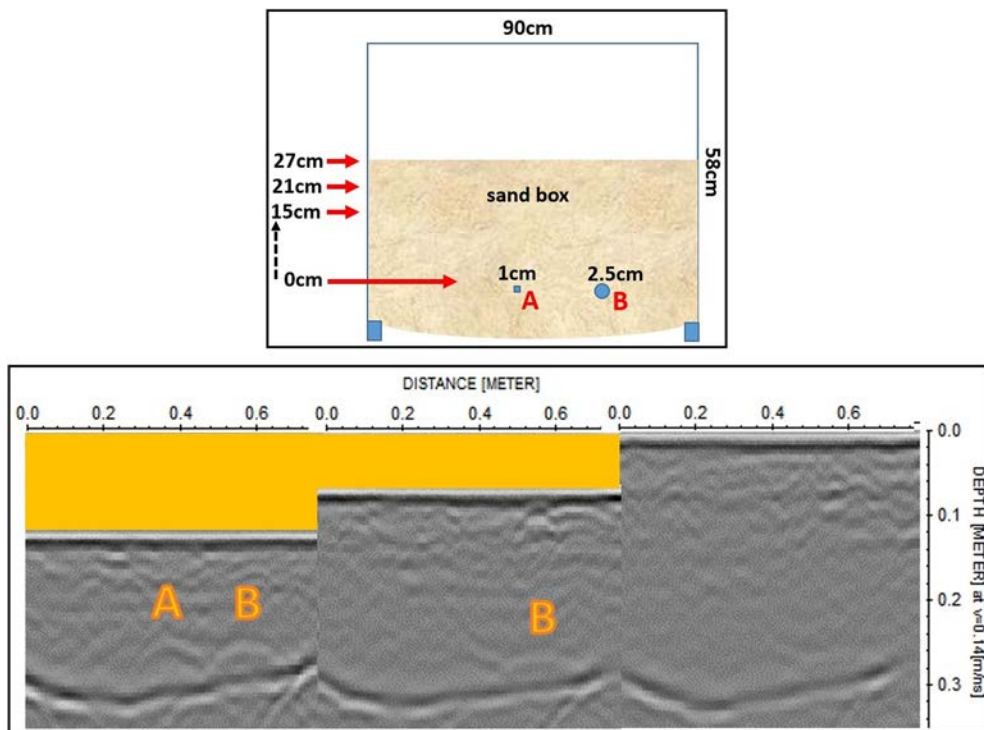

Figure 8
GPR tests on dry sand with VWC = 8%. **A** and **B** are empty targets with a 1 cm square section and a 2.5 cm circular section, respectively. Sand thickness above the targets was progressively increased from 15 cm to about 27 cm. Both targets are detectable at the depth of 15 cm but they gradually disappear as the depth is increased

might detect qanats down to a maximum depth of 8 m assuming a VWC of about 8% for the hosting sand. A comparison of the maximum depth obtained for the scaled frequency 75 MHz in this test with the results discussed for Figs. 5 and 6 shows how rapidly the penetration depth decreases with increasing the VWC. To be rigorous, we have to mention that by increasing the VWC to the levels for which the absorption is not negligible we do not satisfy the lossless assumption that is actually required to extrapolate the laboratory results by simply applying the proper scaling factor. Therefore, these extrapolated detection ranges obtained in moist sand might represent optimistic expectations.

The results of our laboratory tests with a variety of scaling factors are summarized in Table 1. It is observed that a dominance of dry soil in the subsurface allows GPR method to penetrate as deep as a few tens of meters, depending on the frequency of the antenna. This detection range would be more than enough for most qanats with their depth ranging between 5 m and 30 m. However, the penetration depth will considerably decrease as the VWC of the soil and/or clay content of the medium increase.

The general rule that can be derived from Table 1 is presented in Table 2. We can conclude from Table 2 that qanats are detectable at a maximum normalized depth of about 15–17 times of the wavelength in dry sands with VWC < 5%. The best performance (17 wavelengths) was observed with the scaled frequency of 240 MHz while at 90 MHz the maximum normalized depth decreases at 15 wavelengths. This is consistent with the fact that reducing the frequency, we increase the wavelength and thus we reduce the normalized size of the qanat and its scattering width (Radzevicius & Daniels, 2000). Table 2 also shows that the detectable range rapidly decreases to less than 3 or 4 times of the wavelength in moist sands with VWC of about 8%.

The GPR system used for the laboratory tests was an IDS system with a 3 GHz antenna. By extending these results to scaled frequencies we assume that the radar performance figure is not changing with the antenna frequency and by generalizing these results to other GPR brands we assume that the radar performance figure of the most widely used commercial GPRs is quite similar.

4.2. Field Surveys

Figure 9 shows an example of the quality of GPR data for profile 2 that was measured with the

Table 1

Summarized results from the laboratory tests (Figs. 5, 6, 7 and 8) with different scales and their corresponding scaled frequency and penetration depth for dry sand and moist sand (assuming that sand can be considered dry when VWC < 5%)

Linked test (Figure)	Anomaly	Target diameter (cm)	Target depth (cm)	Scaling factor	Scaled frequency (MHz)	Scaled depth (m)	Velocity (cm/ns)	Scaled wavelength (m)
Dry sand (VWC < 5%)								
Figure 5	B	1	30	100	30	30	15.4	5.1
Figure 5	A	1.6	30	62.5	48	19	15.4	3.2
Figure 5	C	2.5	30	40	75	12	15.4	2.1
Figure 6	B	2.5	50	40	75	20	16.5	2.2
Figure 6	A	4	50	25	120	13	16.5	1.4
Figure 7c	A	3	**85**	33.3	90	**28**	16.7	1.9
Figure 7b	A	6	91	16.7	180	15	16.7	0.9
Figure 7a	A	8	**95**	12.5	240	**12**	16.7	0.7
Moist sand (VWC = 8%)								
Figure 8	A	1	**15**	100	30	**15**	14.0	4.7
Figure 8	B	2.5	**21**	40	75	**8**	14.0	1.9

Bold is used to report depths that were proved to be the maximum detectable depths for the corresponding targets

250 MHz antenna. The image shown on Fig. 9 is obtained after time-calibration, filtering, background removal and energy decay compensation. Although some reverberations generated by near-surface targets and some lateral scattering disturb the image, the yellow arrow distinguishes a weak deep signal that might be the diffraction from a qanat. The position of this signal is compatible with the expected qanat mapped by remote sensing studies. The depth to this qanat is about 13 m based on GPR results.

Further processing was performed on the data and the final results are shown in Fig. 10 for all profiles. The images show the envelope of the radar data after migration and after extracting the profile segments that are supposed to intercept the qanat.

Profile 1, which is measured with the 50 MHz antenna, confirms the presence of the qanat at the depth of 13.5 m and the horizontal distance of 116 m along the profile. The subsoil of the study area is dry sand and the velocity of the radar wave in the study

Table 2

Expected maximum depth of detectable qanats in dry sand (VWC < 5%) and moist sand (VWC = 8%)

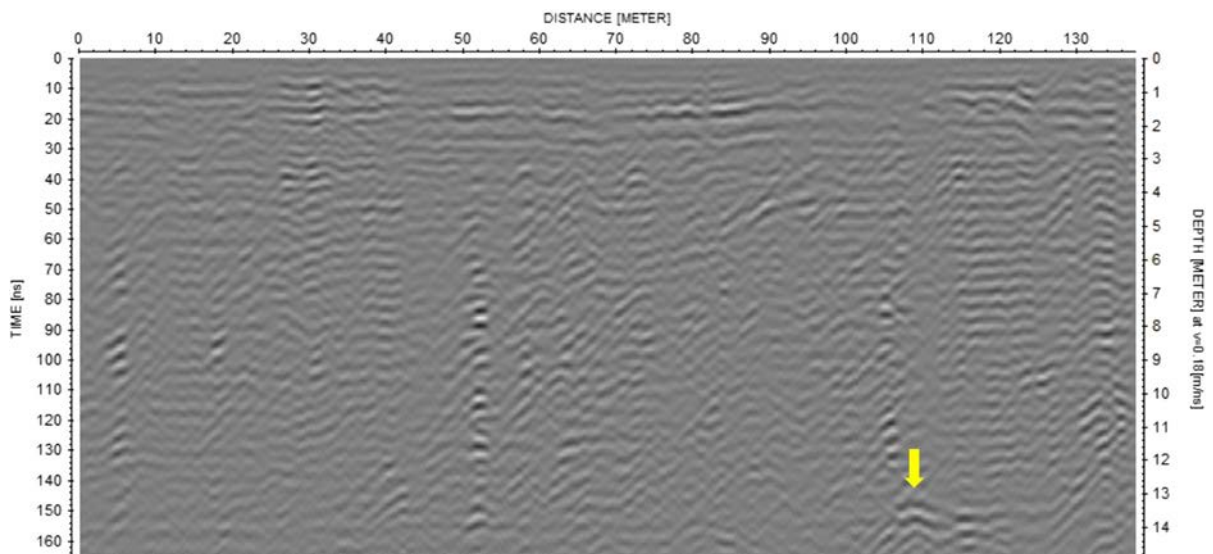| Frequency (MHz)	Maximum penetration depth (m)	Wavelength (m)	Maximum normalized depth (depth/wavelength)
Dry sand (VWC < 5%)			
30	> 30	5.1	> 6
48	> 19	3.2	> 6
75	> 20	2.2	> 9
90	= 28	1.9	= 15
120	> 13	1.4	> 9
180	> 15	0.9	> 16
240	= 12	0.7	= 17
Moist sand (VWC = 8%)			
30	= 15	4.7	< 3
75	= 8	1.9	< 4

Figure 9
An example of GPR data quality for profile 2 measured with the 250 MHz antenna (refer to Fig. 4 for location of GPR profiles)
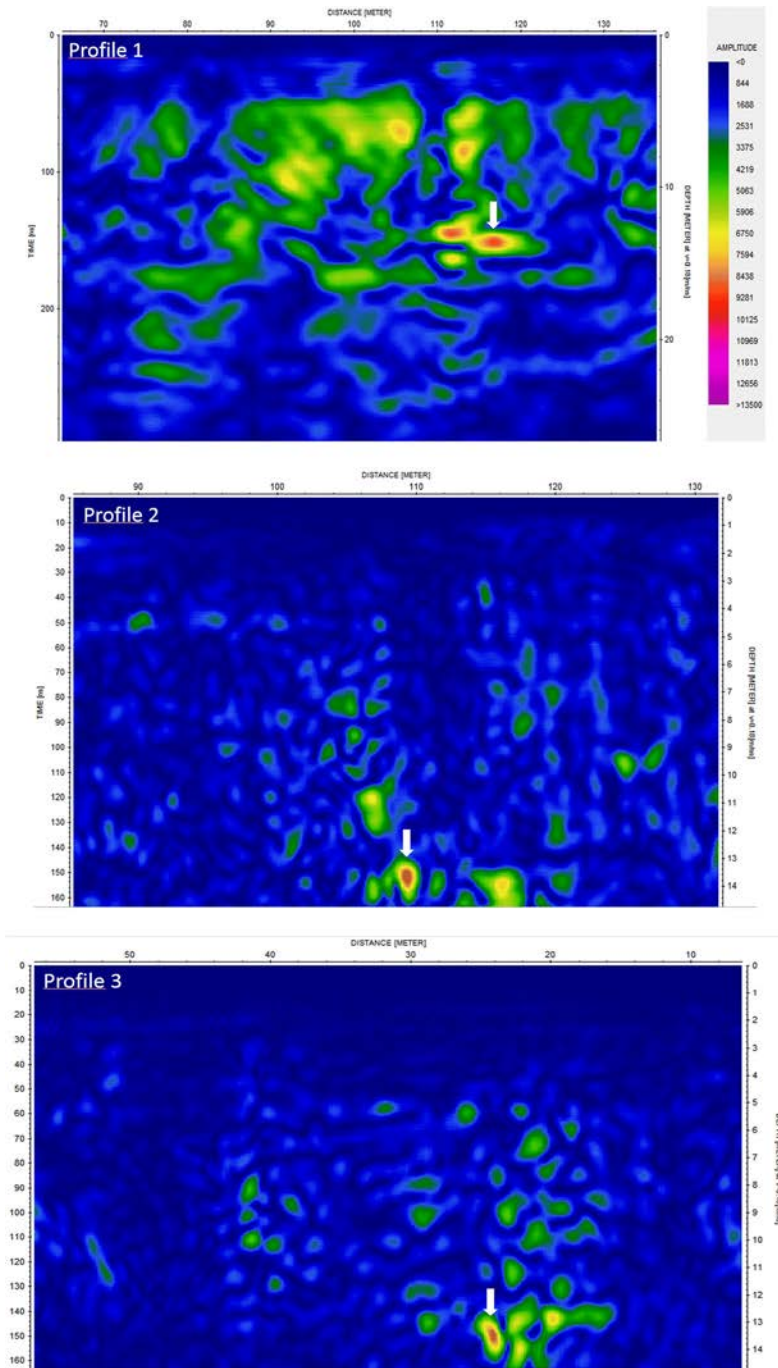
Figure 10
Final GPR images, after migration and envelope extraction (refer to Fig. 4 for location of GPR profiles). The white arrow points to the qanat gallery detected at the depth of 13.5 m

area is estimated to be 0.18 m/ns corresponding to a relative permittivity of about 2.8. This suggests a very dry subsoil and thus a good penetration of the radar wave. With this velocity, the wavelength at 50 MHz is equal to 3.6 m. The results in Table 2 suggest that the maximum normalized depth to be

able to detect a qanat in dry sand is larger than 6 wavelengths for the frequency of 48 MHz. Therefore, with the 50 MHz antenna we expect to detect qanats deeper than 21.6 m in the study area and as demonstrated in Fig. 10, the qanat at the depth of 13.5 m is detected by this antenna despite the presence of a lot of noise, mostly resulting from air wave scattering captured by the unshielded antenna. In conclusion, the result of the profile measured with the 50 MHz antenna is consistent with the results of our laboratory tests summarized in Table 2.

Profiles 2 and 3, which were measured with the 250 MHz antenna, both confirm the presence of the qanat at the depth of 13.5 m and respectively at the horizontal distances of 109 m and 24 m along the profile. Note that these profiles approximately follow the same trajectory but were measured in the opposite direction. Also note that the starting point of profiles 1 and 2 were not exactly the same (profile 2 starting a few meters to the East of the starting point of profile 1). This difference and the expected limited accuracy of the distances measured during the acquisitions are the reasons why the target does not appear at exactly the same distances in profiles 1 and 2. Based on the conclusions from laboratory tests, the maximum normalized detection depth for a qanat in dry sand using a GPR antenna with the frequency of 240 MHz is 17 wavelengths, thus about 12.25 m for the 250 MHz antenna that in a medium with velocity equal to 0.18 m/ns generates a wavelength of 0.72 m. Therefore, we are almost at the detection limit; nevertheless, we could detect the 13.5 m-deep qanat with this antenna thanks to the very favorable hosting material.

5. Conclusions

Our laboratory tests focused on exploring the qanat detection depth achievable with GPR surveys. Results were extrapolated from high frequency measurements by applying the corresponding geometrical scaling factors to both depth and frequency. The results of laboratory tests with a variety of scaling factors showed that:

- Depending on the frequency of the antenna, GPR can detect qanats deep to a few tens of meters in dielectric hosting environments like dry sand;
- The maximum normalized depth for a qanat to be detectable by GPR is about 15–17 wavelengths in favorable material like dry sands (assuming that sand is dry when VWC < 5%);
- The best performances in terms of maximum normalized depth are expected by the highest frequency antennas because a qanat observed with a shorter wavelength produces a higher scattering width;
- In more humid sand (e.g., VWC = 8%) the normalized depth for a qanat gallery rapidly decreases to 3 or 4 wavelengths or even less, considering that when absorption losses are not negligible the scaling approach that we applied to extrapolate laboratory results is not rigorously valid anymore.

The field surveys conducted with the 50 MHz and 250 MHz antennas showed that both antennas detected a scattering target at a depth of about 13.5 m in a position that is compatible with the supposed trajectory of a qanat derived from remote sensing studies. The results are consistent with the predictions derived from the laboratory tests for both frequencies. The qanat depth was largely within the expected detection range for the lower frequency and was a little beyond the predicted detection range of 17 wavelengths (equal to 12.25 m) for the medium frequency. Based on that we can conclude that the 17 wavelengths detection range suggested for dry non-conductive soil should be considered a conservative rule of thumb that in extremely favorable situations might be extended by about 10%.

The results of this work will be used to design the future field surveys planned in the qanat test site at SBUK. By applying a proper scaling factor the results can be also used as a rule of thumb for the selection of the optimal GPR antenna frequency for any similar application (e.g., cavity detection) in arid or semiarid non-conductive soils.

Data availability

Field data of this research are considered sensitive data and cannot be shared publicly. The laboratory data will be available from the authors upon request.

Declarations

Publisher's Note Springer Nature remains neutral with regard to jurisdictional claims in published maps and institutional affiliations.

REFERENCES

Alsharahi, G., Faize, A., Maftei, C., Bayjja, M., Louzazni, M., Driouach, A., & Khamlichi, A. (2019). Analysis and modeling of GPR signals to detect cavities: case studies in Morocco. *Journal of Electromagnetic Engineering and Science, 19*(3), 177–187. https://doi.org/10.26866/jees.2019.19.3.177

Arosio, D., Hojat, A., Munda, S., & Zanzi, L. (2018). High-frequency GPR investigations in San Vigilio Cathedral, Trento. *24th European Meeting of Environmental and Engineering Geophysics, Porto.* https://doi.org/10.3997/2214-4609.201802545

Arosio, D., Hojat, A., Munda, S., & Zanzi, L. (2020). Non-destructive root mapping: Exploring the potential of GPR. *3rd Asia Pacific Meeting on Near Surface Geoscience & Engineering, Chiang Mai, Thailand.* https://doi.org/10.3997/2214-4609.202071057

Benedetto, A., Tosti, F., Ciampoli, L. B., & D'amico, F. (2017). An overview of ground-penetrating radar signal processing techniques for road inspections. *Signal Processing, 132*, 201–209. https://doi.org/10.1016/j.sigpro.2016.05.016

Beres, M., Luetscher, M., & Olivier, R. (2001). Integration of ground-penetrating radar and microgravimetric methods to map shallow caves. *Journal of Applied Geophysics, 46*, 249–262. https://doi.org/10.1016/S0926-9851(01)00042-8

Conyers, L. B. (2013). *Ground-penetrating radar for archaeology* (3rd ed.). AltaMira Press.

Francke, J., & Utsi, V. (2009). Advances in long-range GPR systems and their applications to mineral exploration, geotechnical and static correction problems. *First Break, 27*, 85–93.

Goblot, H. (1979). Les Qanats, une technique d'acquisition de l'eau/English: Qanat a technique for obtaining water, Paris-La Haye, Mouton/Ecole des hautes en sciences sociales, 236 P. Translated from French to Persian by A. Sarvqad Moqadam, M. H. Papoli Yazdi, 1992.

Harun, A. R., & Samsudin, A. R. (2014). Application of gravity survey for geological mapping and cavity detection: Malaysian case studies. *EJGE, 19*, 8247–8259.

Hojat, A., Zanzi, L., Loke, M. H., Ranjbar, H., & Karimi Nasab, S. (2018). Integration of geoengineering techniques to map hidden qanats at Shahid Bahonar University of Kerman. *24th European Meeting of Environmental and Engineering Geophysics, Porto.* https://doi.org/10.3997/2214-4609.201802529

Hojat, A., Izadi Yazdanabadi, M., Karimi-Nasab, S., Arosio, D., & Zanzi, L. (2019a). GPR method as an efficient NDT tool to characterize carbonate rocks during different production stages. *2nd Asia Pacific Meeting on Near Surface Geoscience and Engineering, Kuala Lumpur, Malaysia.* https://doi.org/10.3997/2214-4609.201900394

Hojat, A., Zanzi, L., Karimi-Nasab, S., Ranjbar, H., & Loke, M. H. (2019b). Laboratory and field GPR measurements to detect qanats. *10th International Workshop on Advanced Ground*

Penetrating Radar, The Hague, Netherlands. https://doi.org/10.3997/2214-4609.201902571

Hojat, A., Loke, M. H., Karimi Nasab, S., Ranjbar, H., & Zanzi, L. (2020). Two-dimensional ERT simulations to compare different electrode configurations in detecting qanats. *3rd Asia Pacific Meeting on Near Surface Geoscience & Engineering, Chiang Mai, Thailand.* https://doi.org/10.3997/2214-4609.202071056

Hojat, A., Ferrario, M., Arosio, D., Brunero, M., Ivanov, V. I., Longoni, L., Madaschi, A., Papini, M., Tresoldi, G., & Zanzi, L. (2021). Laboratory studies using electrical resistivity tomography and fiber optic techniques to detect seepage zones in river embankments. *Geosciences, 11*(2), 69. https://doi.org/10.3390/geosciences11020069

Hojat, A., Zanzi, L., Ranjbar, H., Karimi Nasab, S., & Loke, M. H. (2023). An opportunity to directly observe qanat galleries at depth and test electrical resistivity tomography surveys. *5th Asia Pacific Meeting on Near Surface Geoscience & Engineering, Taipei, Taiwan.* https://doi.org/10.3997/2214-4609.202378054

Izadi-Yazdanabadi, M., Hojat, A., Zanzi, L., Karimi-Nasab, S., & Arosio, D. (2022). Analytical models and laboratory measurements to explore the potential of GPR for quality control of marble block repair through resin injections. *Applied Sciences, 12*(3), 987. https://doi.org/10.3390/app12030987

Kobori, I. (1964). Some considerations on the origin of the Qanat system. In: Memorial collected papers dedicated to Prof. E. Ishida. Tokyo.

Kofman, L., Ronen, A., & Frydman, S. (2006). Detection of model voids by identifying reverberation phenomena in GPR records. *Journal of Applied Geophysics, 59*, 284–299.

Levanon, N. (1988). *Radar principles.* John Wiley & Sons Ltd.

Loke, M. H., Chambers, J. E., Rucker, D. F., Kuras, O., & Wilkinson, P. B. (2013). Recent developments in the direct-current geoelectrical imaging method. *Journal of Applied Geophysics, 95*, 135–156.

Lyu, Y. Z., Wang, H. H., & Gong, J. B. (2020). GPR detection of tunnel lining cavities and reverse- time migration imaging. *Applied Geophysics.* https://doi.org/10.1007/s11770-019-0831-9

Maierhofer, C., & Leipold, S. (2001). Radar investigation of masonry structures. *NDT & E International, 34*(2), 139–147. https://doi.org/10.1016/S0963-8695(00)00038-4

Mochales, T., Casas, A. M., Pueyo, E. L., Román, M. T., Pocoví, A., Soriano, M. A., & Ansón, D. (2008). Detection of underground cavities by combining gravity, magnetic and ground penetrating radar surveys: A case study from the Zaragoza area, NE Spain. *Environmental Geology, 53*, 1067–1077.

Park, M. K., Park, S., Yi, M. J., Kim, C., Son, J. S., Kim, J. H., & Abraham, A. A. (2014). Application of electrical resistivity tomography (ERT) technique to detect underground cavities in a karst area of South Korea. *Environmental Earth Sciences, 71*, 2797–2806. https://doi.org/10.1007/s12665-013-2658-7

Porzucek, S., & Loj, M. (2021). Microgravity survey to detect voids and loosening zones in the vicinity of the mine shaft. *Energies, 14*(11), 3021. https://doi.org/10.3390/en14113021

Radzevicius, S. J., & Daniels, D. J. (2000). Ground penetrating radar polarization and scattering from cylinders. *Journal of Applied Geophysics, 45*, 111–125.

Rousset, D., Genthon, P., Perroud, H., & Se´ne´chal, G. (1998). Detection and characterization of near surface small karstic cavities using integrated geophysical surveys. *4th Meeting of Environmental and Engineering Geophysical Society.* https://doi.org/10.3997/2214-4609.201407122

Semsar Yazdi, A. A., & Labbaf Khaneiki, M. (2017). *Qanat knowledge: Construction and maintenance.* Springer.

Tresoldi, G., Hojat, A., & Zanzi, L. (2020). G.RE.T.A. installations for real-time monitoring of irrigation dams and canals. *Procedia Environmental Science, Engineering and Management, 7*(2), 271–276.

Valle, S., & Zanzi, L. (1998). Traveltime radar tomography for NDT on masonry and concrete structures. *European Journal of Environmental and Engineering Geophysics, 2*(3), 229–246.

www.unesco.org/, last visited on 15 January 2021.

Zanzi, L., Hojat, A., Ranjbar, H., Karimi Nasab, S., Azadi, A., & Arosio, D. (2019). GPR measurements to detect major discontinuities at Cheshmeh-shirdoosh limestone quarry, Iran. *Bulletin of Engineering Geology and the Environment, 78*(2), 743–752. https://doi.org/10.1007/s10064-017-1153-x